Journal of Molecular Structure 1318 (2024) 139193

Contents lists available at ScienceDirect

Journal of Molecular Structure

journal homepage: www.elsevier.com/locate/molstr

Amelioration potential of synthetic oxime chemical cores against multiple sclerosis and Alzheimer's diseases: Evaluation in aspects of *in silico* and *in vitro* experiments

Anil Yilmaz [a,1,*], Murat Koca [b,1], Selami Ercan [c,2], Ozden Ozgun Acar [d,2], Mehmet Boga [e], Alaattin Sen [f,g], Adnan Kurt [h]

[a] Department of Pharmaceutical Chemistry, Faculty of Pharmacy, Trakya University, Edirne, Turkiye
[b] Department of Pharmaceutical Chemistry, Faculty of Pharmacy, Adiyaman University, Adiyaman, Turkiye
[c] Department of Chemistry, Faculty of Arts and Sciences, Batman University, Batman, Turkiye
[d] Health Services Vocational School of Higher Education, Pamukkale University, Denizli, Turkiye
[e] Department of Analytical Chemistry, Faculty of Pharmacy, Dicle University, Diyarbakir, Turkiye
[f] Department of Molecular Biology and Genetics, Faculty of Life and Natural Sciences, University of Abdullah Gul, Kayseri, Turkiye
[g] Department of Biology, Faculty of Arts & Sciences, Pamukkale University, Denizli, Turkiye
[h] Department of Chemistry, Faculty of Science & Letters, Adiyaman University, Adiyaman, Turkiye

ARTICLE INFO

Keywords:
anti-Alzheimer
Anticholinesterase
In silico
In vitro
Multiple sclerosis
Oxime

ABSTRACT

Alzheimer disease (AD) and multiple sclerosis (MS) are inflammatory neurological disorders. The main symptom of AD is dementia, and the main symptoms of MS are vertigo, sexual dysfunction, cognitive problems, and fatigue. Today, millions of people are affected by AD and MS, and the number is growing day by day. However, there are not any accurate remedies for both disorders. For this reason, discovering novel drug molecules against neurological disorders such as AD and MS is essential and precious. Oximes and benzofurans exhibit many pharmacological effects including anti-inflammatory and neurological activities. Thus, several novel compounds bearing oxime and benzofuran chemical cores were designed and synthesized, and their *in vitro* anticholinesterase activities were investigated in our previous study. A number of the synthesized molecules showed excellent anticholinesterase activity against both AChE and BChE enzymes. The mentioned study constituted a background for this study. In this study, we picked different chemical skeletons among all the synthesized molecules to conduct further *in silico* and *in vitro* experiments. In order to support our *in vitro* anticholinesterase findings, we also examined *in silico* anti-Alzheimer activity of the selected molecules. In addition, *in silico* and *in vitro* activities against MS disease of the synthesized molecules were investigated. Molecule **4** extraordinarily showed outstanding activity against AD disease both *in silico* and *in vitro*, as well as *in silico* activity against MS disease. This feature makes molecule **4** a possible drug lead molecule which is very limited in the market. On the other hand, molecule **1**, a less substituted oxime skeleton, demonstrated the strongest *in vitro* activity against MS disease through *in vitro* anti-inflammatory effect. As an observation, molecule **4** was determined to be the most promising molecule to focus on in the further steps.

1. Introduction

The most prevalent neurodegenerative ailment in elderly adults is Alzheimer's disease (AD), for which there is no known cure. AD already affects more than 35 million individuals globally, which is expected to rise in the near future [1]. Loss of memory, lack of motivation, language issues, a lack of self-care routine, mood changes, and bodily malfunctions are some of the signs of AD [2,3].

The exploration of cholinesterase enzyme inhibitors intending to enhance the acetylcholine levels is the main focus for the studies on the

* Corresponding author: Department of Pharmaceutical Chemistry, Faculty of Pharmacy, Trakya University, 22030, Edirne, Turkiye.
E-mail address: anilyilmaz@trakya.edu.tr (A. Yilmaz).
[1] Anil Yilmaz and Murat Koca contributed equally to this work and should be considered as co-first authors.
[2] Selami Ercan and Ozden Ozgun Acar contributed equally to this work and should be considered as co-second authors.

https://doi.org/10.1016/j.molstruc.2024.139193
Received 9 April 2024; Received in revised form 30 June 2024; Accepted 2 July 2024
Available online 3 July 2024

treatment of AD [4-6]. The cholinergic impact is a hypothesis related to levels of neurotransmitter acetylcholine in the neurons. Studies are focused on inhibiting the designated enzymes (AChE and BChE) by designing of new synthetic molecules [7,8]. Two cholinesterase enzymes, acetylcholinestrease (AChE) and butyrylcholinesterease (BChE) hydrolyze the neurotransmitter acetylcholine [9].

Arachidonic acid is converted into prostaglandins (PGs), thromboxanes, and prostacyclin, which act as chemical mediators of inflammation, by the heme-containing enzyme cyclooxygenase (COX). While COX-2 (inducible form) is overexpressed within inflammatory cells and the central nervous system in both acute and chronic inflammatory conditions, COX-1 (constitutive form) is responsible for the synthesis of PG and thromboxane in many cells, including those in the intestinal tract, kidneys, and blood platelets [10]. Additionally, research has shown that COX-2 is overexpressed in a variety of human malignancies, including breast and gastric cancer [11,12].

The most widely used pharmaceuticals for treating chronic inflammatory diseases, pain, and fever are non-steroidal anti-inflammatory drugs (NSAIDs), which work by blocking COX enzymes (the arachidonic acid pathway) to stop the production of PGs and other inflammatory mediators [13]. The FDA granted valdecoxib, celecoxib, and rofecoxib approval for clinical use as NSAIDs with enhanced gastrointestinal safety among selective COX-2 inhibitors [14]. However, because of the cardiovascular issues that they induce, valdecoxib and rofecoxib were later taken off the market. The researchers have been inspired to investigate and assess other templates with specific COX-2 inhibitory activity [15] because of their unfavorable cardiovascular side effects. Research on the creation of selective COX-2 inhibitors is still being drawn by the discovery of new and selective COX-2 inhibitors in cancer chemotherapy and neurological illnesses, including Parkinson's and Alzheimer's [15,16].

The family of 11 distinct isoenzymes known as phosphodiesterases (PDEs) catalyzes the hydrolysis of the two secondary signaling molecules cyclic adenosine monophosphate (cAMP) and cyclic guanosine monophosphate (cGMP) [17]. Accordingly, 6 PDEs are divided into three groups: those that operate on both cAMP and cGMP, as well as those that are (i) specific to cAMP, (ii) unique to cGMP, and (iii) both. Due to their exclusive involvement in controlling of cAMP levels, phosphodiesterase 4 (PDE4) enzymes fall within the first category. When PDE4 is blocked, the resulting increase in intracellular cAMP levels triggers the activation of particular protein phosphorylation cascades, which in turn causes the inflammatory cells to exhibit various functional responses, such as the inhibition of TNFα synthesis. Four genes encode the four PDE4 subtypes (PDE4A–PDE4D) [18].

A substantial sphingolipid known as sphingosine 1-phosphate (S1P) functions as an intracellular second messenger and is essential for the regulation of angiogenesis, motility, vascular stability, and blood-brain barrier permeability [19,20]. By controlling the movement of T- and B-cells, it is also connected to the immune system [21]. Multiple sclerosis (MS) is a condition of the central nervous system (CNS) that is brought on by an increase in the S1P gradient in T-cells' cell membranes [21]. Three enzymes work together to control the amount of sphingosine 1-phosphate (S1P) in the cell, including sphingosine kinase (SK), sphingosine phosphates, and sphingosine 1-phosphate lyase (S1PL) [22].

A prospective therapeutic target for developing new chemical scaffolds to treat inflammatory illnesses including MS and AD is S1PL, a member of the group II decarboxylase family. T-cell migration from lymph nodes into the CNS is inhibited by S1PL inhibition due to an increase in intracellular S1P levels [23,24]. When S1PL is lacking, cellular amyloid protein buildup, the primary cause of AD, is reduced. The activity of APP and -secretases is decreased by S1PL inhibition, which has a beneficial impact on AD [25]. S1PL is also implicated in tumor-suppressor pathways and cancer pathway surveillance [26], and it has been demonstrated that S1PL inhibition increases survival after cardiac arrest in organisms lacking SK [27]. Additionally, rheumatoid arthritis patients have responded well to S1PL inhibition, which prevents lymphocyte migration [28,29]. Here, utilizing an integrated computational strategy, our goal is to discover new S1PL inhibitors.

An autoimmune disease known as MS causes demyelinating lesions in the white and grey matter of the central nervous system (CNS) [30]. According to recent studies, oxidative stress is a novel etiological element contributing to the pathogenesis of MS. Impaired oxidant/antioxidant balances, in particular glutathione peroxidase 4 (GPx4), a neuronal antioxidant enzyme in charge of eliminating harmful peroxide phospholipids, are one of the causes of oxidative stress. By preventing ferroptosis, which is iron-dependent cell death and has recently been linked to a number of disorders [31,32], GPx4 plays a crucial role in neurodegeneration. Additionally, MS patients have decreased expression of this vital antioxidant enzyme [33]. Therefore, GPx4 deficiency makes people more vulnerable to the ferroptotic process, which uses GPx4 to catalyze the transformation of polyunsaturated fatty acids into hazardous lipid hydroperoxides. Due to the buildup of these harmful lipids brought on by GPx4 loss, neuronal cell structure may be harmed, ultimately resulting in cell death [34,35].

In our previous study, we synthesized some novel molecules bearing benzofuran and oxime moieties, and investigated their anti-Alzheimer activity through *in vitro* evaluation of their inhibition capacity against cholinesterase enzymes. We obtained very promising results [36]. AD and MS are both neurological disorders and have similar properties, such as neuro-inflammation which is the common outcome for almost all neurological diseases. Thus, we decided to investigate the *in vitro* activity of these synthesized molecules against MS. In addition, in order to support *in vitro* findings, we also comprehensively carried out *in silico* examinations against both AD and MS diseases. For that purpose, we selected some of the synthesized molecules bearing different chemical skeletons possessing *in vitro* anticholinesterase activities at various levels to reveal which chemical framework is more potent against either AD or MS *in silico* and *in vitro* perspectives [36]. We studied several parameters *in vitro* anti-MS activity using SH-SY5Y cell lines through inflammation/chemokine/cytokine, myelination/demyelination and apoptosis/cell adhesion. In *in silico* studies, we investigated the binding properties of those synthesized molecules in AChE and BChE enzyme structures as anti-Alzheimer, in COX-2 and PDE4 enzyme structures as anti-inflammatory, and in S1PL and GPx4 enzyme structures as anti-multiple sclerosis. *In silico and in vitro* studies revealed that the synthesized molecules could have inhibition effects for all the mentioned enzyme structures.

2. Materials and methods

Data related to synthesis, characterization and *in vitro* anticholinesterase activity methods of the synthesized compounds exist in the study published by Yilmaz et al. in 2023 [36].

2.1. Preparation of protein structures and ligands

Prior to docking studies 2D structures of ligands were drawn by utilizing MarvinSketch [37] program and converted to 3D structures by the aim of DS Visualizer program [38]. Then, ligands were forwarded to quantum mechanics calculation in order to obtain their optimized structures. Thus, the optimizations of ligands were started with semi-empirical AM1 [39,40] method and followed by using DFT method with the B3LYP/6–31+*g*(d,p) [41,42] level of theory.

We have investigated anti-Alzheimer, anti-inflammatory and anti-multiple sclerosis properties of the ligands by performing molecular docking studies against drug targets of these diseases. Thither, we have used crystal structures of acetylcholinesterase (AChE) (PDB ID: 4EY7 [43]), butyrylcholinesterase (BChE) (PDB ID: 6QAA [44]) as anti-Alzheimer drug targets, crystal structures of cyclooxygenase-2 (COX-2) (PDB ID: 3LN1 [45]), phosphodiesterase 4 (PDE4) (PDB ID: 4WCU [19]) as anti-inflammatory drug targets, crystal protein

structures of sphingosine 1-phosphate lyase (S1PL) (PDB ID: 4Q6R [46]) and glutathione peroxidase-4 (GPx4) (PDB ID: 2OBI [47]) as MS drug targets. The crystal protein structures of drug targets obtained through PDB databank (www.rcsb.org) [48] and optimized ligands were prepared for docking studies with MGL Tools program [49]. Following removing of all unneeded residues and water molecules, polar hydrogens and Gasteiger charges were added to amino acid residues.

We have taken advantage of co-crystalized structures of the ligands to identify the binding sites of each protein, apart from 2OBI crystal protein structure which does not include a co-crystalized ligand. Therefore, the binding site of this protein was defined through the binding site residues as included in literature [47]. The coordinates and dimensions of grid boxes of proteins are given in Supplementary Materials Table S1. Docking studies were performed as explained in the literature [50].

2.2. Cell culture

The human neuroblastoma cell line SH-SY5Y was purchased from the American Type Culture Collection (ATCC, USA). The cells were cultured in DMEM-F12 supplemented with 10 % FBS and 1 % penicillin/streptomycin mixture in a humidified atmosphere of 95 % air with 5 % CO^2 at 37 °C and were subcultured twice a week.

2.3. Cytotoxicity assay

SH-SY5Y cells were seeded in 96-well plates at a density of 1×10^3 cells/ml culture medium. After 24-h incubation, the cells were treated with varying concentrations (ranging from 1 μM to 200 μM) of compounds **1–4**. An equal amount of medium without compound was added to untreated cells (control). Treated and control cells were incubated for 24 h at 37 °C in a humidified 5 % CO_2 atmosphere. Following incubation, the medium was replaced by 0.5 % crystal violet solution (w/v; in 50 % Ethanol). Dye absorbed by live cells was extracted with sodium citrate (0.1 M in 50 % ethanol). Absorbance was read at 630 nm. Viability was expressed as a percentage of the control, untreated cells.

2.4. RNA isolation and cDNA synthesis

Total RNA was extracted from SH-SY5Y cells using an RNeasy Plus mini kit (Qiagen) with slight modifications according to the manufacturer's instructions. Elution was performed with 40 mL RNase-free water. After elution, the RNA concentration was determined using a Nanodrop (MaestroNano micro-volume Spectrophotometer, USA), and the RNA was reverse transcribed using Easy Script cDNA Synthesis Kit (ABM). The reaction mixture was incubated for 50 min at 50 ºC, followed by termination by heating at 85 ºC for 5 min. cDNA was stored at −80ºC for further use [51].

2.5. Quantitative RT-PCR

Quantitative Real-Time PCR (qRT-PCR) analysis was performed using 2X SYBR Green qPCR Master Mix (ABM) in an Exicycler 96 Real-Time Quantitative Thermal Block PCR System (Bioneer, Daejeon, Korea) for each gene. The mRNA levels of genes (APP, CCL5, CXCL9, CXCL10, GFAP, HIF1A, IL6, MAG, MMP9, NF-κB1, PLP, PTPN11, STAT3, SOD, TNFα) were determined by qRT-PCR. Beta-actin was chosen from the group of housekeeping genes as the minor varying reference gene. The qPCR using custom-designed primers for the genes is listed in Table 1 [51].

2.6. Statistical analysis

The QIAGEN PCR Array Data Analysis Web Portal (version 3.5) was used to analyze the qPCR data. The p-values are computed by applying a Student's *t*-test, specifically utilizing a two-tail distribution and assuming equal variances across the two samples. This test is performed on the replicate $2^{-\Delta\Delta Ct}$ values for each gene in each treatment group, comparing them to the control group. In order to conduct statistical analyses, it is necessary to calculate the $2^{-\Delta\Delta Ct}$ value for each gene in each sample, and then these values were import into the Minitab 13 statistical software package (Minitab Inc. State College, PA, USA). Comparison between groups was made using Student's *t*-test, and $p < 0.05$ was selected as the level required for statistical significance.

3. Results and discussion

Results and discussion related to synthesis, characterization and *in vitro* anticholinesterase activity of the synthesized compounds (Fig. 1) can be found in the study published by Yilmaz et al. in 2023 [36].

Prior to performing docking studies of ligands, the validity of the docking method was tested by re-docking of co-crystallized ligands to the protein structures (Fig. 2). Since glutathione peroxidase-4 (2OBI) does not contain a ligand in the crystal structure as mentioned before the binding site of this protein was defined through the literature [47]. Thus, we could not perform any validation procedure for it. The RMSD values between superimposed co-crystalized ligand and their docking structures are acceptable (Fig. 2) [52,53].

3.1. In silico experiments

As represented in Fig. 3, ligands are successfully subjected to the binding sites of proteins.

The analysis of docking results exposed that ligands are mostly have

Table 1
Primer sequences of the selected human genes.

GeneBank	Gene	F_Sequence (5′->3′)	R_Sequence(5′->3′)	Tm
NM_000484	APP	GCCCTGCGGAATTGACAAG	CCATCTGCATAGTCTGTGTCTG	61ºC
NM_002985	CCL5	CAGTCGTCTTTGTCACCCGA	AGAGCAAGCAGAAACAGGCA	62ºC
NM_002416	CXCL9	GGCTCTTTCCTGGCTACTCC	TCCCTGGTCCCTGTAGTGAG	61ºC
NM_001565	CXCL10	ACCAGAGGGGAGCAAAATCG	GGAAGTGATGGGAGAGGCAG	62ºC
NM_002055	GFAP	GTGTCAGAAGGCCACCTCAA	TCAGGTCTGGGGAAATGTGC	62ºC
NM_001530	HIF1A	GGCGCGAACGACAAGAAAAA	GTGGCAACTGATGAGCAAGC	61ºC
NM_000600	IL6	ACTCACCTCTTCAGAACGAATTG	CCATCTTTGGAAGGTTCAGGTTG	59ºC
NM_002361	MAG	CCAAGTAGTCCACGAGAGCTT	CAGGTCCCCACGGAAGTAGT	62ºC
NM_004994	MMP9	GGGACGCAGACATCGTCATC	TCGTCATCGTCGAAATGGGC	62ºC
NM_003998	NFKB1	TCGCGCTGAGTATAAAAGCC	GGCAAAGTTTCGTGGATGCG	61ºC
NM_000533	PLP	GAAAGCCCTTTTCATTGCAGGA	GGCTAGTCTGCTTTGTGGCT	56ºC
NM_002834	PTPN11	GACGTTCCCAAAACCATCCA	TCTTCTTCAATCCTGCGCTGT	56ºC
NM_003150	STAT3	AACAGGATGGCCCAATGGAA	GAAGCGGCTATACTGCTGGT	61ºC
NM_000454	SOD	TAAAGTAGTCGCGGAGACGG	CTTCGTCGCCATAACTCGCT	62ºC
NM_000594	TNF	TGGGATCATTGCCCTGTGAG	GGTGTCTGAAGGAGGGGGTA	62ºC
NM_001101	ACTB	GCCGCCAGCTCACCAT	GATGCCTCTCTTGCTCTGGG	59ºC

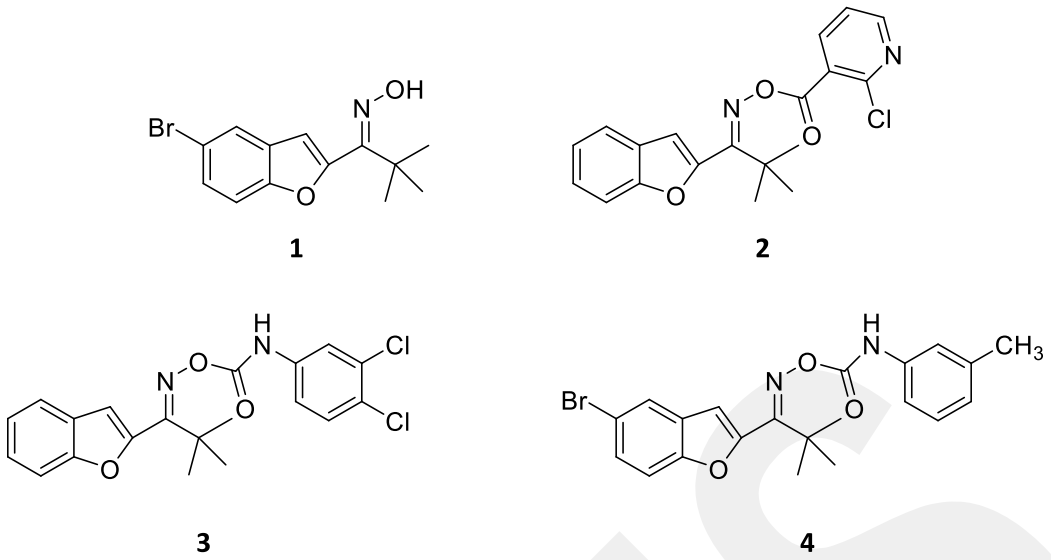

Fig. 1. Synthesized chemical cores.

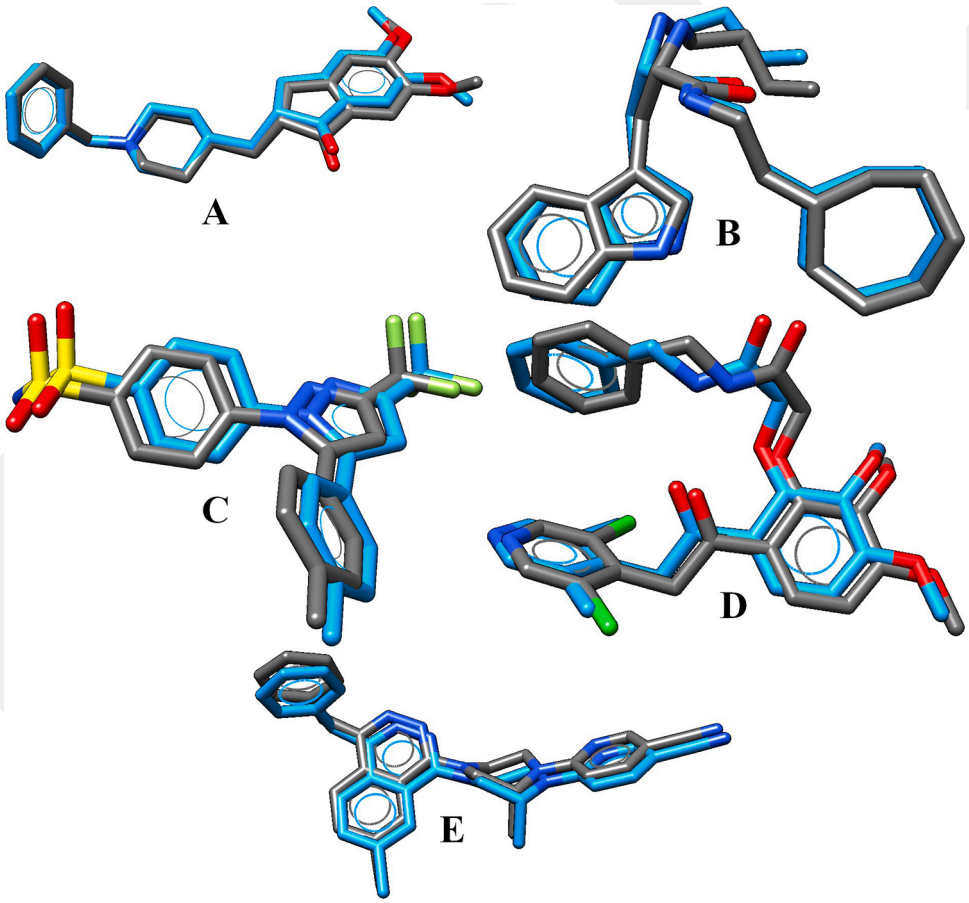

Fig. 2. Superimposed co-crystalized and docked structures of ligands in protein structures. Carbon atoms of co-crystalized structures of ligands are colored as blue while carbon atoms of docked structures of ligands are colored as gray. A) Ligand included in 4EY7 (AChE protein, RMSD: 1.140), B) Ligand included in 6QAA (BChE protein, RMSD: 0.879), C) Ligand included in 3LN1 (COX-2 protein, RMSD: 0.651), D) Ligand included in 4WCU (PDE4 protein, RMSD: 0.737) and E) Ligand included in 4Q6R (S1PL protein, RMSD: 0.565).

better binding properties for AChE enzyme rather than BChE enzyme which are taught to participate in treatment of Alzheimer disease (AD). Ligand coded as **4** has the best binding free energy value of −10.68 kcal/mol for the AChE enzyme and −8.59 kcal/mol for the BChE enzyme (Table 2).

The anti-inflammatory effects of ligands were tested on COX-2 and PDE4 enzymes. Where ligand **2** seems to have the best inhibition effect on the COX-2 enzyme with a binding free energy score of −9.58 kcal/

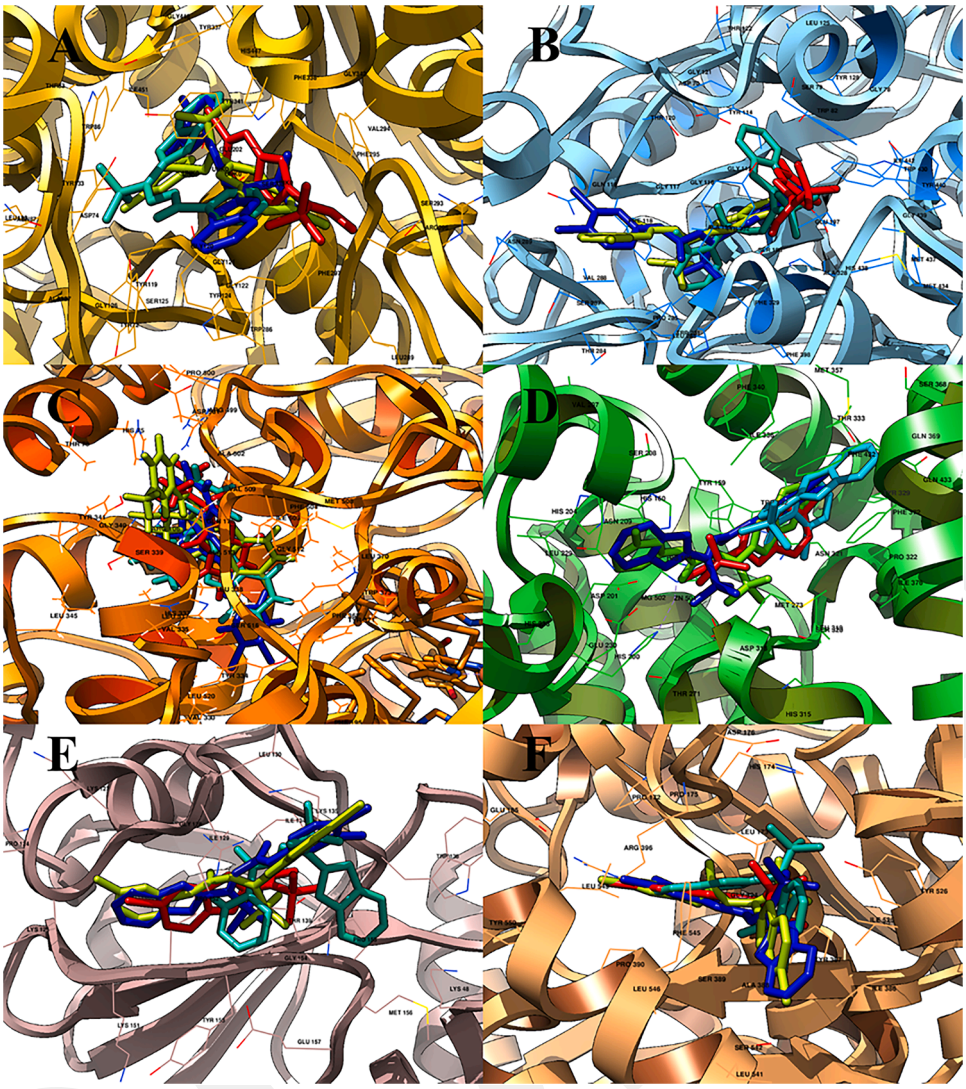

Fig. 3. Representation of the binding modes of ligands in the binding site of proteins (Residue atoms in a distance of 4 Å to ligands are depicted as line). A) AChE, B) BChE, C) COX-2, D) PDE4, E) GPx4, F) S1PL. Ligands are colored as folowing: Ligand 1: blue, Ligand 2: cyan, Ligand 3: chartreuse, Ligand 4: red).

Table 2
Binding free energy values of ligands in proteins (kcal/mol).

	4EY7 (AChE)	6QAA (BChE)	3LN1 (COX-2)	4WCU (PDE4)	4Q6R (S1PL)	2OBI (GPx4)
1	−9.07	−7.01	−8.32	−7.95	−7.98	−6.26
2	−9.31	−8.41	−9.58	−8.58	−7.98	−6.03
3	−10.08	−8.16	−7.00	−8.19	−9.45	−7.54
4	−10.68	−8.59	−7.08	−9.06	−10.56	−6.67

mol, the ligand **4** has a binding free energy value of −9.06 kcal/mol against the PDE4 enzyme (Table 2). The results showed that ligands have better binding properties for the GPx4 enzyme rather than the S1PL enzyme. Ligand **3** gave the best binding free energy value of −7.54 kcal/mol for GPx4 and the ligand **4** gave a binding free energy value of −10.56 kcal/mol for binding S1PL enzyme (Table 2).

The ligand **4** which has best binding properties in the binding site of AChE enzyme placed in the anionic site of the enzyme by creating many hydrophobic interactions such as π-σ, pi/amide-pi stacked/T-shaped and π-alkyl interactions. The ligand's benzofuran, phenyl rings and methyl parts of ligand involved in these interactions. While ligand creates mentioned hydrophobic interactions with anionic site residues of AChE enzyme Trp86, Gly120, Gly121, Tyr124, Trp286, Tyr337, Phe338, and Tyr341, it makes many van der Waals interactions, including both anionic and esteratic site residues (Figs. 4-A and B). Among the ligands, where **2** creates only hydrophobic and van der Waals interactions as ligand **4, 3** forms one hydrogen bond via its amide oxygen with the phenolic hydrogen atom of Tyr14 residue (Fig. 4), and **1** forms two hydrogen bonds via nitrogen and hydrogen atoms of hydroxylamine group with Phe295 backbone HN atom and Ser293 hydroxyl oxygen (Fig. 4), respectively. It has been defined that all ligands are located at an anionic site where **2, 3** and **4** ligands interact with esteratic residues, since ligand **1** is a small molecule in comparison with other ligands it does not interact with esteratic site residues (SM Figure S1-S3).

The interactions between the ligands and binding site of BChE were determined through the anionic sites residues Asn68, Ile69, Asp70, Gly78, Trp82, Gly439, Tyr440 Gly116, Gly117, Thr120, Trp231, Pro285, Leu286, Val288, Ala328, Tyr332, Trp430, Met437 and the esteratic site residues Ser287, Ser198, His438, Gln119, Ser79, Phe398, Phe329.

The best binding ligand for BChE was the ligand **4**. Although the ligand has few hydrophobic and hydrogen bond interactions with enzyme residues (Fig. 5A), it interacts with many residues via van der Waals interactions (Fig. 5B). The ligand creates two hydrogen bonds via benzofuran ring oxygen with Gly117 backbone HN atom and via amide hydrogen with Pro285 backbone oxygen atom. Other ligand interactions

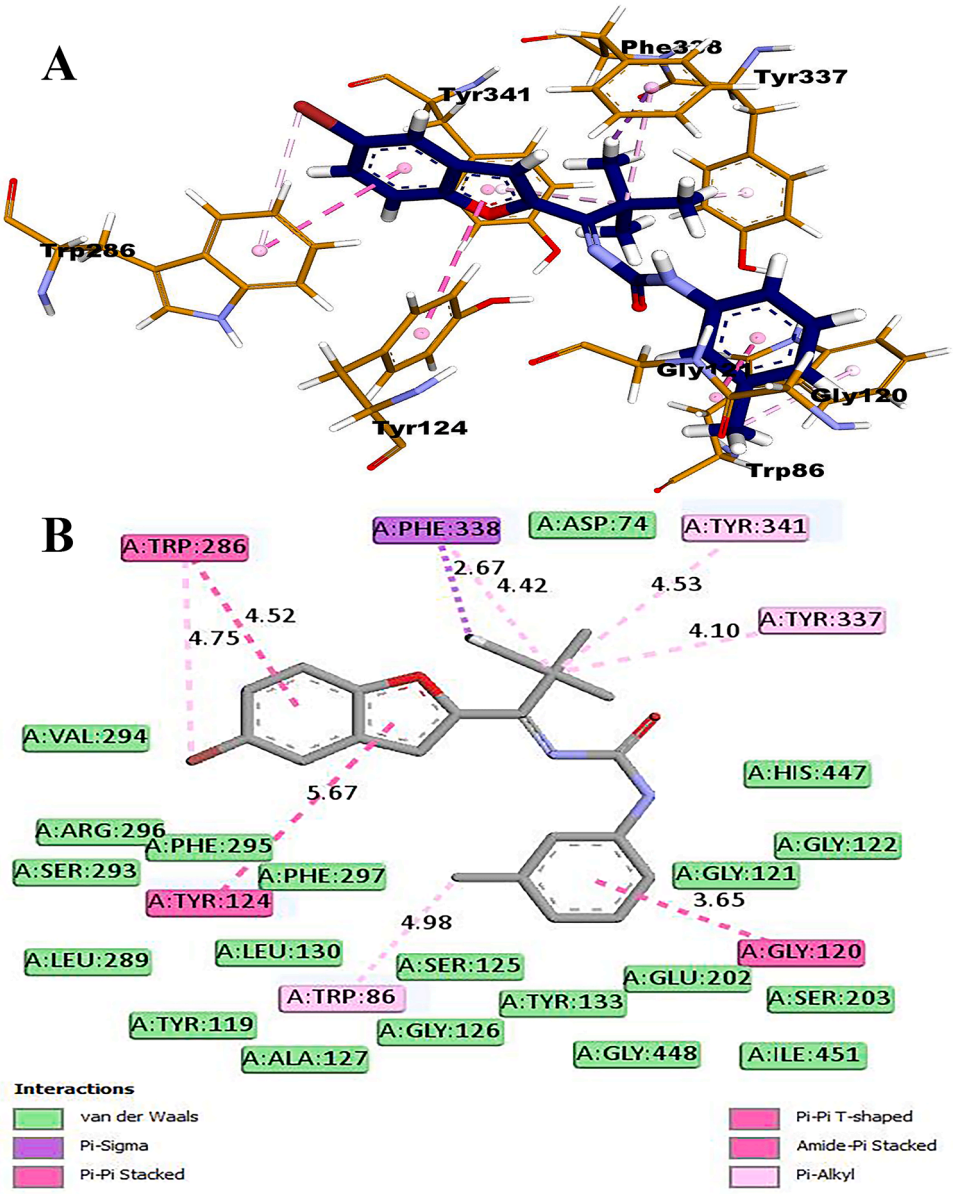

Fig. 4. 3D representation of ligand 4-AChE (4EY7.pdb) interactions. Carbon atoms of ligand (thick) are depicted as dark blue and carbon atoms of residues (thin) are colored as yellow (A). 2D representation of ligand 4-AChE (4EY7.pdb) interactions with interaction distances (B).

are hydrophobic type interactions such as π-pi T shaped (with His438) and π-alkyl interactions (with Trp82 and His438). Where **3** (SM Figure S4), **2** (SM Figure S5) and **4** ligands have hydrophobic and van der Waals interactions with both anionic site and esteratic site residues, ligand **1** makes both interactions with anionic site residues, but only van der Waals interactions with esteratic residues (SM Figure S6).

The binding free energy values of ligands to the COX-2 (3ln1.pdb) and PDE4 (4wcu.pdb) enzymes were also hopeful. Through the ligands **2** and **4** were the best binding ligands for COX-2 and PDE4 enzymes, respectively. The docking scores of ligands were defined as −9.58 kcal/mol for **2** and −9.06 kcal/mol for **4**. Ligand **2** forms a π-cation interaction via pi electrons of the pyridine group with NH1 group of Arg499 guanidine. Besides, the ligand's alkyl methyl atoms create alkyl-alkyl interactions with Val335 and Ala513 residues. All other ligand interactions are π-alkyl type interactions in which pi electrons of interactions mediated through pyridine and benzofuran atoms. The alkylic side of these interactions is provided by Val335, Leu338, Ala513, Arg499, Ala502, and Val509 residues of the enzyme (Fig. 6A). While the 2D representation of **2**-COX-2 interactions is depicted in Fig. 6B, 2D representations of other ligands' interactions are given SM Figure S7-S9. The analyzes indicate that beside having similar hydrophobic interactions of **2**, each of **4** and **1** ligands form two hydrogen bonds with residues Leu338, Arg499 and Gln178, and Phe504, respectively (Figs. 6-A and B and SM Figure S8,S9).

The binding site of PDE4 enzyme (4WCU.pdb) includes Mg^{2+} and Zn^{2+} ions. Analyzes revealed that where ligands **1, 3** and **4** interact with one or both of these ions, **2** does not create any interaction with these ions. The best binding ligand **4** has two unfavorable bumps and also a metal-acceptor type interaction with Mg^{2+} ion. While phenyl and benzofuran rings of ligand contribute interactions via pi electrons, methyl groups and bromine atom of ligand assist the ligand-protein interactions via alkylic interactions. Ligand creates π-pi T shaped interactions with His160 and His204, alkyl-alkyl interactions with Leu319 and Leu229, and π-alkyl interactions with Tyr329, Phe372, Ile336 and Leu229 residues (Figs. 7-A and B). The detailed 2D interaction images of the other ligands are given in SM Figure S10–12. Among four ligands, there is only one hydrogen bond seen which is formed by ligand **1** with His160 residue (SM Figure S12).

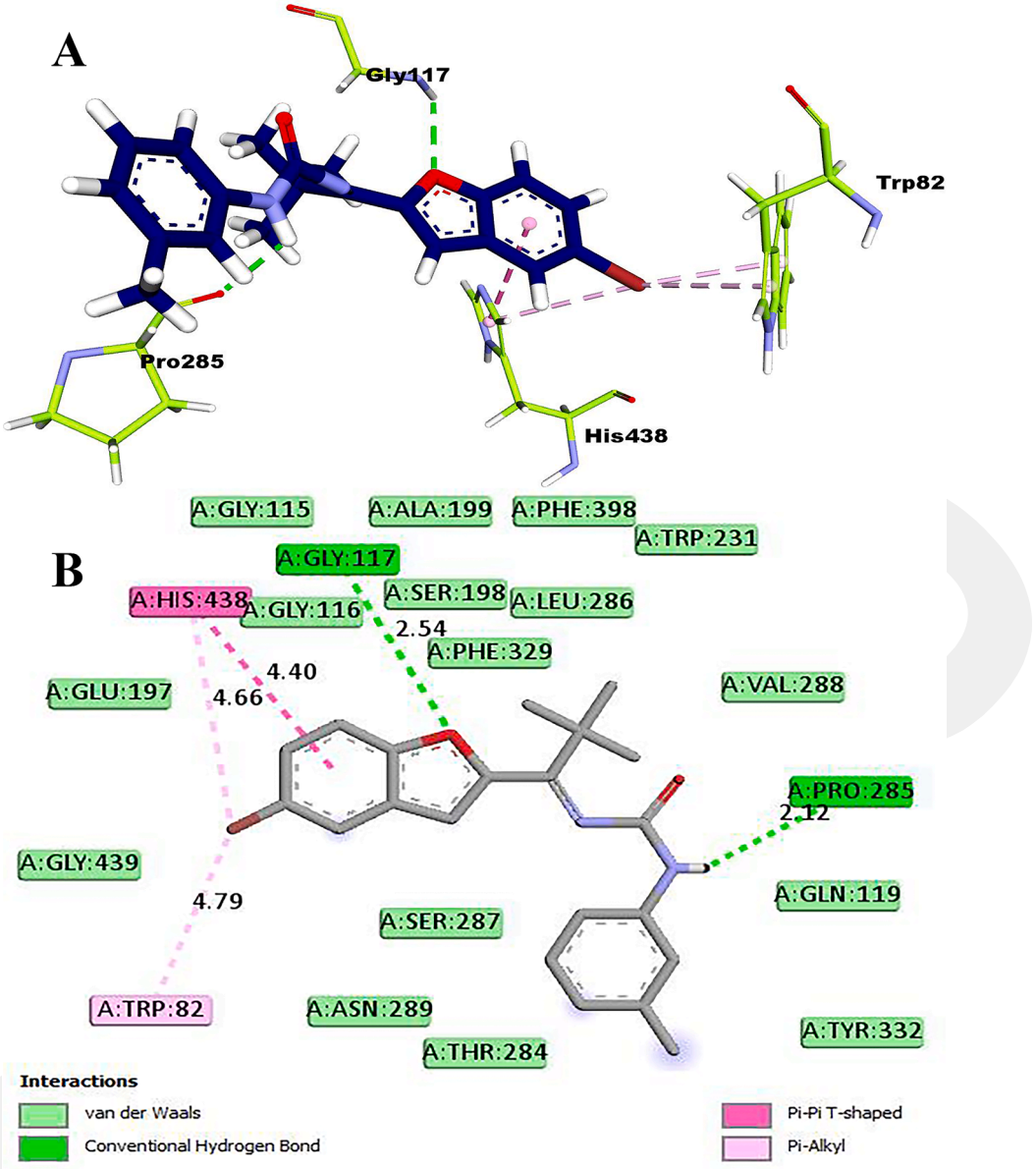

Fig. 5. 3D representation of ligand **4**-BChE (6QAA.pdb) interactions. Carbon atoms of ligand (thick) are depicted as dark blue and carbon atoms of residues (thin) are colored as chartreuse (**A**). 2D representation of ligand **4**-BChE (6QAA.pdb) interactions with interaction distances (**B**).

Two different targets were chosen to test the inhibition effects of molecules against MS disease. One of them was the S1PL enzyme crystal structure (4Q6R.pdb), which is also used as an AD disease target [30], and the second one was the crystal structure of the GPx4 enzyme. The analyzes indicated that the interactions between four ligands and protein residues are mostly hydrophobic (Figs. 8-A and B and SM Figures S13-S15). As with AChE, BChE and PDE4 enzyme structures, ligand **4** showed the best binding properties for S1PL enzyme structure. The ligand gave a binding score of −10.56 kcal/mol. Hydrogen bond formed between the amide hydrogen of the ligand and the backbone oxygen of Ala388 is one of the valuable interactions between ligand and protein. Other interactions are π-pi stacked, alkyl-alkyl and π-alkyl type interactions in which phenyl and benzofuran rings of ligand serve as pi electron source and where methyl groups and bromine support alkylic interactions. Among the residues, Phe545 serves pi electrons for π-pi stacked type interaction. Other remainder Leu541, Ile386, Leu549, Pro172, Pro390, Ala388, Ala388 and Leu173 residues are taken charge in alkylic interactions (Figs. 8-A and B).

Ligand **3** has a binding score of −7.54 kcal/mol in the binding site of the crystal structure of the GPx4 enzyme (2OBI.pdb). The ligand creates a hydrogen bond with Lys135 residue via its amide oxygen and a π-lone pair interaction with Lys127 via benzofuran ring pi electrons. The chlorine atom of the ligand makes alkyl-alkyl interactions with alkyl parts of Leu130 and Lys135 residues, benzofuran and phenyl rings of ligands serve in providing pi electrons for π-alkyl interactions formed with alkyl parts of Ile129, Arg152, Leu130, and Lys135 residues (Figs. 9-A and B). The interaction analyses of other ligands indicate that ligand **2** creates two hydrogen bonds with Ile129 and Lys135 residues, ligand **1** forms three hydrogen bonds with Lys135, Thr139 and Arg152 residues, while ligand **4** does not create hydrogen bonds (SM Figure S16-S18).

3.2. *In vitro anti-MS effect results*

It was primarily aimed to determine the non-toxic doses of these compounds in SH-SY5Y cells. In preclinical toxicology studies, EC_{05} and EC_{10} (the doses lethal to 5 % and 10 % of cells treated) represent a safe phase I trial starting doses. For this reason, EC_{05} and EC_{10} doses for **1, 2, 3** and **4** in human neuroblastoma cells were investigated by crystal violet

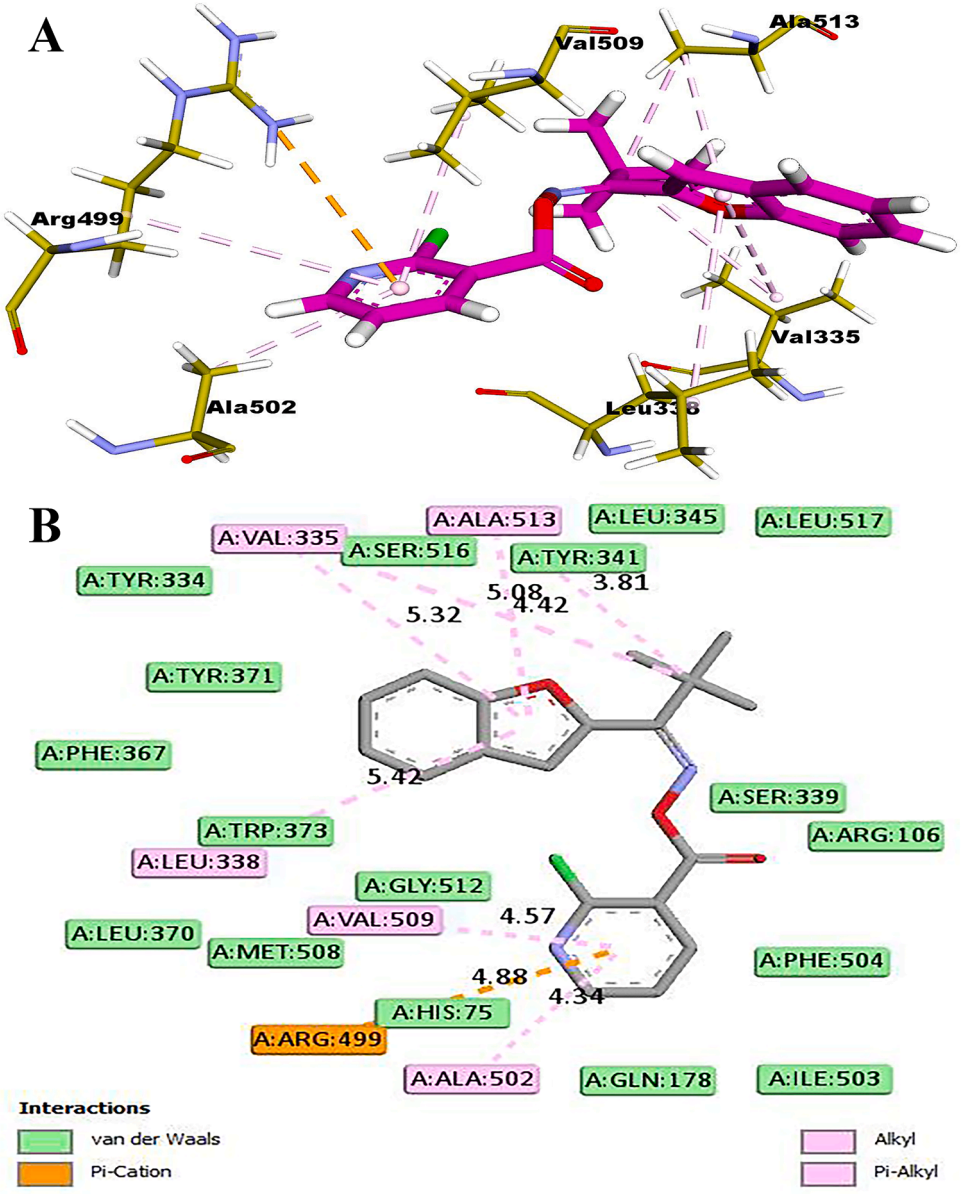

Fig. 6. 3D representation of ligand **2**-COX-2 (3LN1.pdb) interactions. Carbon atoms of ligand (thick) are depicted as magenta and carbon atoms of residues (thin) are colored as olive (**A**). 2D representation of ligand **2**-COX-2 (3LN1.pdb) interactions with interaction distances (**B**).

staining. EC05 and EC10 values for the compounds were calculated in SH-SY5Y cells at 24 h (Table 3).

The effect of molecules **1, 2, 3** and **4** on the expression of the selected genes essential in the neuroinflammation was determined in SH-SY5Y cells (Table 4).

Cycle threshold (Ct) values were used to calculate fold-changes in mRNA abundance using the $2^{-\Delta\Delta Ct}$ method [54]. Changes in mRNA expression levels for the evaluated genes were compared between the EC05 and EC10 doses and the control group, with the mRNA expression level set to 1 in the control group.

Myelin associated glycoprotein (MAG) and proteolipid protein (PLP) are the main myelin proteins, and that are essential for myelination/remyelination [55]. These genes were not significantly altered in any of the different compounds. Proinflammatory or inflammatory cytokines/chemokines such as CCL5, CXCL9, CXCL10, IL6, HIF1A, and TNF-α play a vital role in the pathogenesis of neuroinflammation such as MS [56]. Most of these genes are regulated by transcription factor nuclear factor κB (NF-κB). NF-κB plays a significant role in inflammatory diseases such as MS by regulating immunity and inflammation [57].

Matrix metalloproteinases are zinc-containing endopeptidases. MMP9 contributes to the disease's pathogenesis by improving the deterioration of the blood-brain barrier and inflammation of the CNS [58]. SOD (superoxide dismutase) is an enzyme that scavenges reactive oxygen species, and its expression is reported to be suppressed in MS patients [56,59]. Statistically, significant changes in the expression of 10, 9, 6 and 6 genes were detected in the treatment with molecules **3, 2, 4** and **1**, respectively.

With the application of compound **3**, CCL5, IL6, NFKB, PTPN11 expressions significantly increased at dose EC_{10}; at dose EC_{05}, HIF1A and APP increased 2.2 and 2.3 fold respectively. In addition, a significant increase in the expressions of STAT, TNF, SOD and GFAP were also observed in both doses. While CCL5 expression increased 5.2 folds with the application of EC10 **2** treatment, CXCL9, CXCL10, and MMP9 increased 2.1, 2 and 2.3-folds at EC05 dosage, respectively. IL6, NFKB, STAT3, TNF and GFAP are genes whose expressions were significantly increased at both doses of EC_{05} and EC_{10} with the treatment **2**. CCL5 and CXCL10 increased by 2.08 and 4.1 folds with the application of **4** at dose EC_{10}, respectively; GFAP expression increased 2.4 fold at dose EC_{05}.

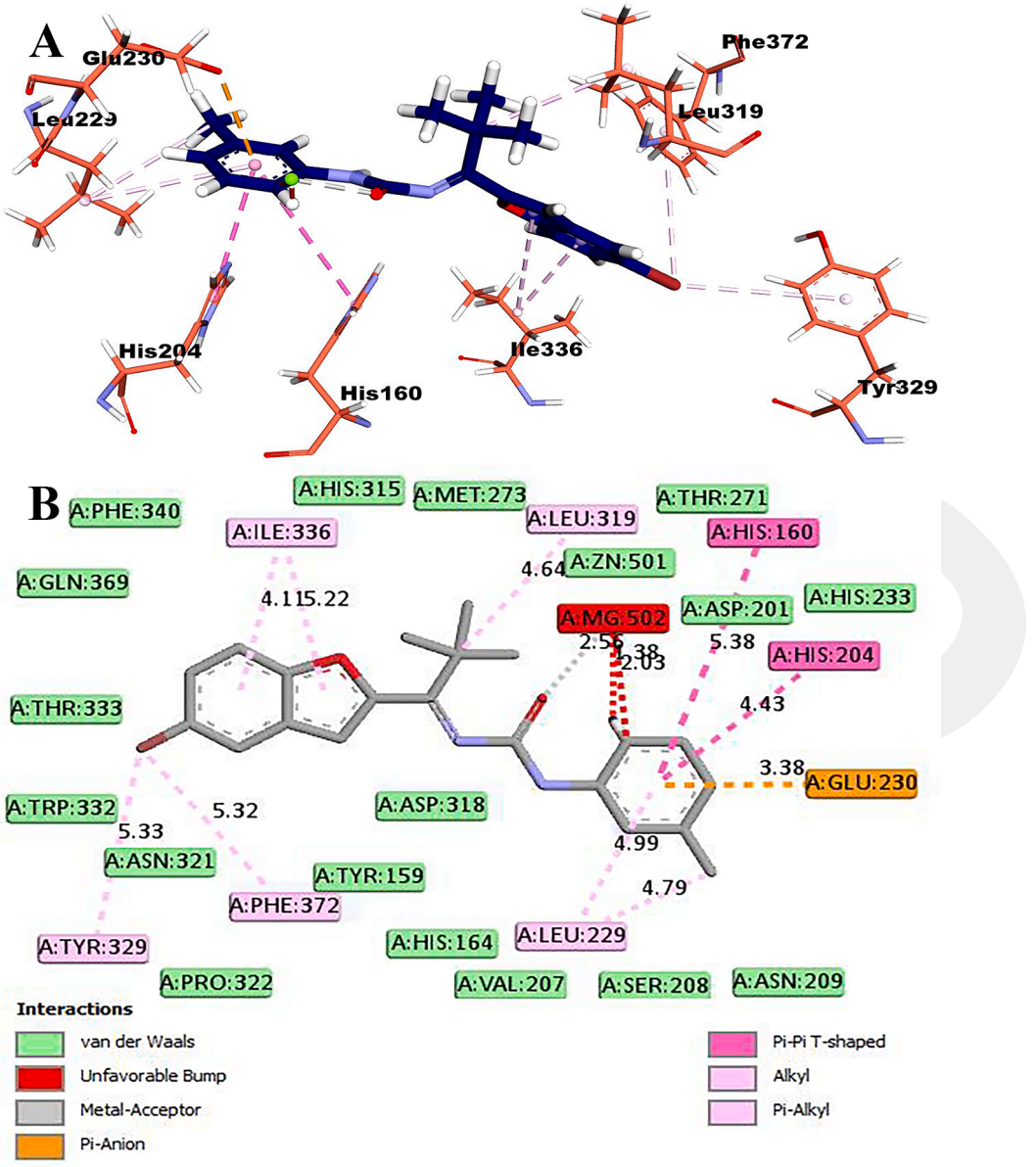

Fig. 7. 3D representation of ligand **4**-PDE4 (4WCU.pdb) interactions. Carbon atoms of ligand (thick) are depicted as magenta, and carbon atoms of residues (thin) are colored as tomato (**A**). 2D representation of ligand **4**-PDE4 (4WCU.pdb) interactions with interaction distances (**B**).

Also, CXCL9 and TNF mRNA levels increased significantly in both doses of the compound **4**. At EC_{10} dosage of compound **1**, CXCL9, CXCL10, PTPN11, TNF and GFAP mRNA expression levels decreased significantly by 4.8, 7.0, 2.3, 2.3, and 2.7 folds, respectively. Also, MMP9 mRNA expression level decreased 2.1 fold at a low dosage and 3.3 fold at a high dosage application. From these data, we can express that compound **1** has a potential anti-inflammatory effect, but further experiments are needed to clarify the anti-inflammatory potential of **1** comprehensively.

Compounds bearing oxime and benzofuran moieties demonstrate several pharmacological effects, including neurological effects, which makes these compounds target drug lead molecules. In our previous published study, numerous novel oxime compounds were synthesized, and their anticholinesterase activity was examined [36]. According to the results, we provided some new very potent molecules possessing anticholinesterase activity, which is even better than the reference drug galantamine, already use in the market.

In order to support and prove our *in vitro* study results, we decided to go further with detailed *in silico* experiments. For this purpose, we selected four molecules bearing different skeleton types to determine which chemical framework is more promising. Molecule **4** showed strong anti-Alzheimer activity through *in silico* ligand-enzyme interactions for both AChE and BChE enzymes. This data supports *in vitro* anticholinesterase activity of the molecule **4**. Molecule **4** highly inhibited both AChE and BChE *in vitro* [36]. This correlation between *in silico* and *in vitro* biological activities is very precious.

Neuro-inflammation is one of the most common symptoms in almost all neurological disorders. Our synthesized molecules showed outstanding anticholinesterase activities which is related to AD, so we concluded that we should investigate both the *in silico* and *in vitro* anti-MS effects of the selected chemical skeletons. Inflammation plays crucial role in MS disease. Thus, the pharmacological effects of the synthesized molecules against MS disorder were examined through anti-inflammatory activity. Molecule **4** exhibited very good *in silico* activity against MS disorder in two parameters (PDE-4 and S1PL). Molecule **4** extraordinarily showed excellent activity against AD disease both *in silico* and *in vitro*, as well as *in silico* activity against MS disease. This feature makes molecule **4** a possible drug lead molecule which is very limited in the market. On the other hand, molecule **1**, a less substituted

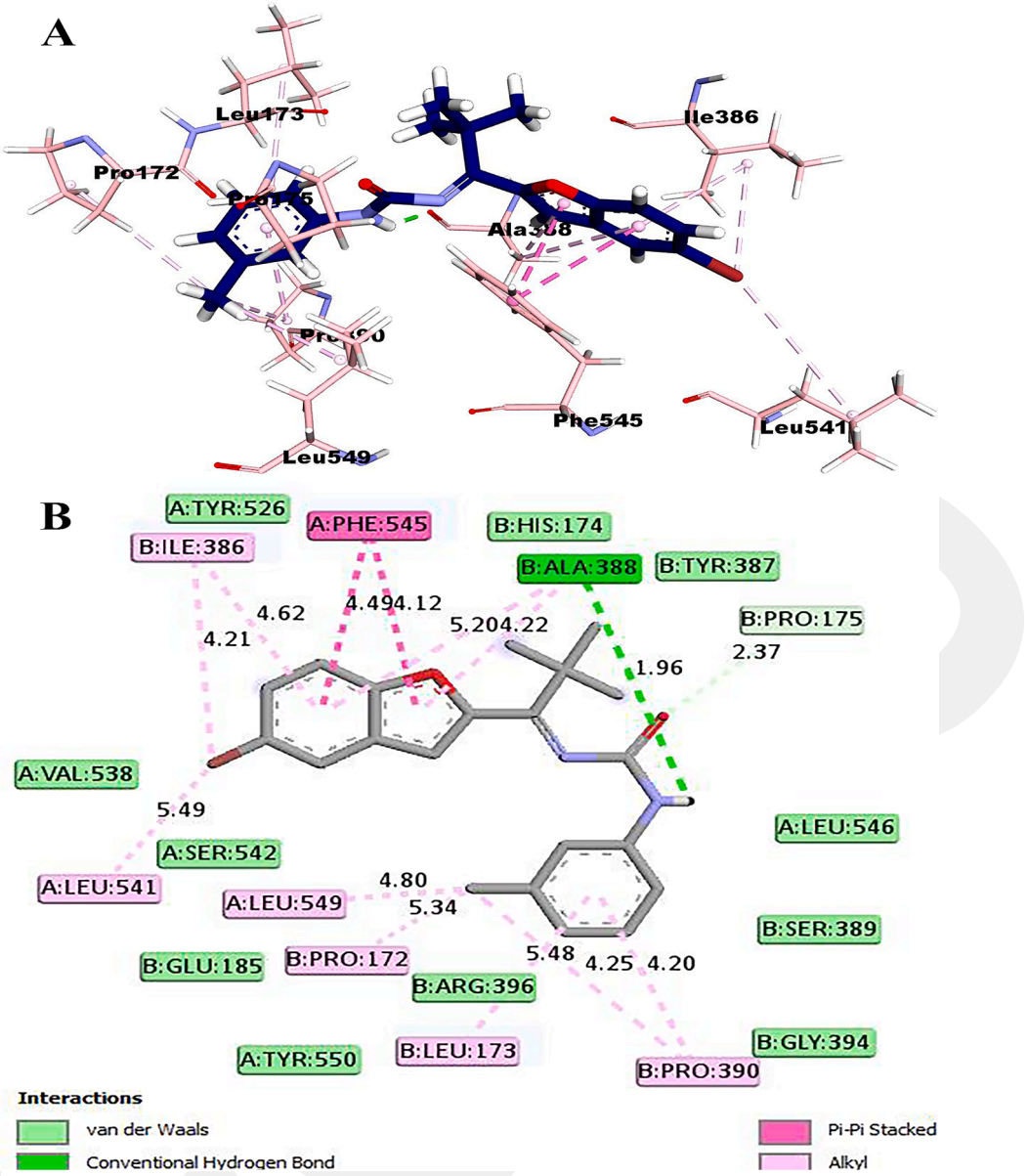

Fig. 8. 3D representation of ligand **4**-S1PL (4Q6R.pdb) interactions. Carbon atoms of ligand (thick) are depicted as magenta and carbon atoms of residues (thin) are colored as pink (**A**). 2D representation of ligand **4**-S1PL (4Q6R.pdb) interactions with interaction distances (**B**).

oxime skeleton, demonstrated the strongest *in vitro* activity against MS disease through *in vitro* anti-inflammatory effect. As an observation, molecule **4** was determined to be the most promising molecule to be focused on for further steps in the drug development against neurological disorders such as AD and MS.

4. Conclusion

It is obvious from the literature that nitrogen-containing compounds exhibit various biological activities including neurological effects. In addition, in our recent publication, many novel oximes were synthesized, and their *in vitro* anticholinesterase activity was investigated. Based on the results, we revealed several potent compounds having anticholinesterase activity [36]. The resulted biological features of those molecules proved a solid background in the structure-activity relationship (SAR) against neurological disorders. Thus, in order to support and prove our *in vitro* study results, we decided to go further with detailed *in silico* experiments. For this purpose, we selected four molecules bearing different skeleton types to determine which chemical framework is more promising. Molecule **4** showed perfect anti-Alzheimer activity through *in silico* ligand-enzyme interactions for both AChE and BChE enzymes. This data supports the *in vitro* anticholinesterase activity of molecule **4**. Molecule **4** highly inhibited both AChE and BChE *in vitro* [36]. This correlation between *in silico* and *in vitro* biological activities is very precious. Neuro-inflammation is common for the most neurological diseases. So, we also examined the anti-MS effect of the selected synthesized molecules via *in silico* and *in vitro* assays. Molecule **4** exhibited very good *in silico* activity against MS disorder in two parameters (PDE-4 and S1PL). Molecule **4** extraordinarily showed awesome *in silico* and *in vitro* anticholinesterase activity, besides *in silico* activity against MS disease. This feature makes molecule **4** a possible drug lead molecule which is an urgent need in the market. On the other hand, molecule **1**, a less substituted oxime skeleton, demonstrated the strongest *in vitro* activity against MS disease through *in vitro* anti-inflammatory effect. As an observation, molecule **4** was determined to be the most promising molecule to be focused on for further studies. This is the first study that comprehensively reveals anticholinesterase and anti-MS activities of the newly synthesized oxime cores through *in silico* and *in vitro* perspectives.

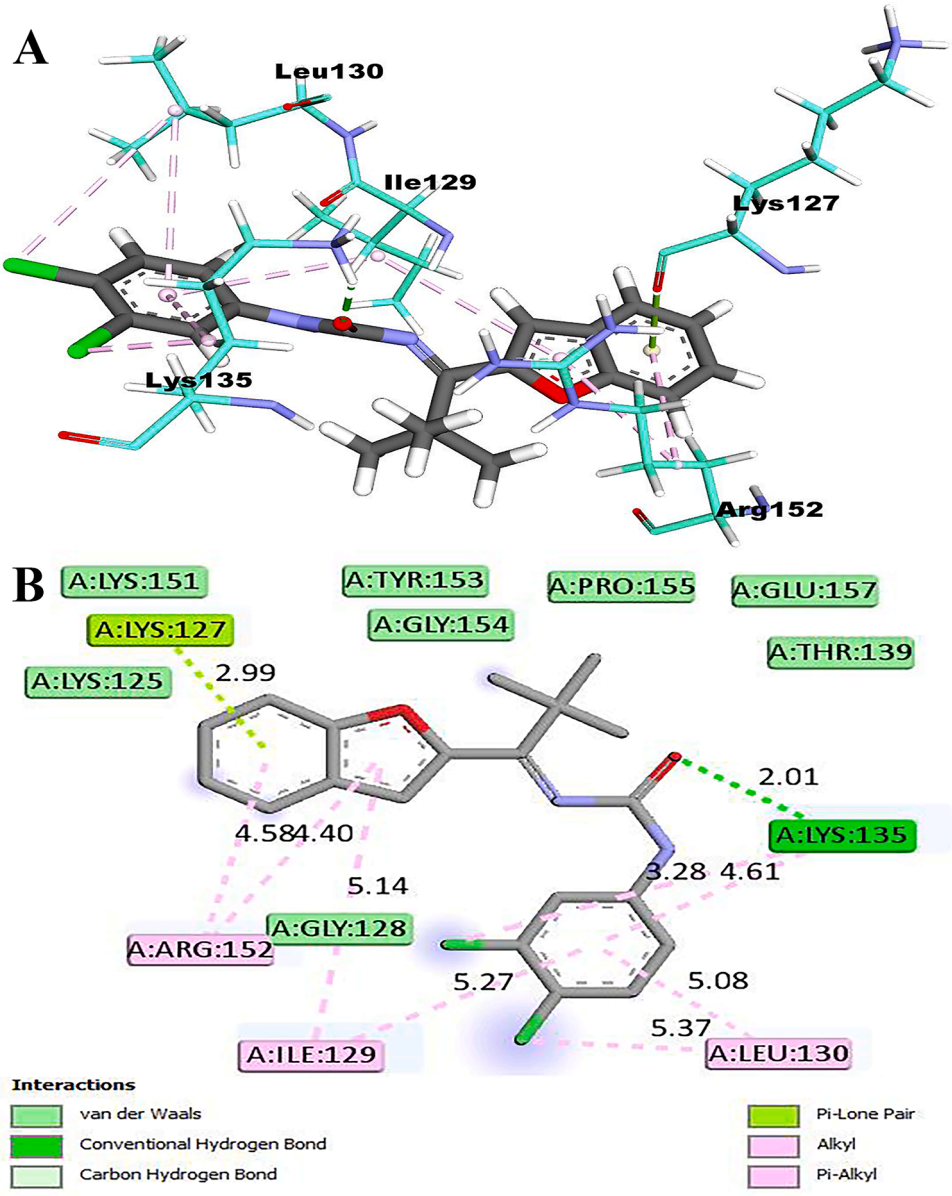

Fig. 9. 3D representation of ligand 3-GPx4 2OBI.pdb) interactions. Carbon atoms of ligand (thick) are depicted as magenta and carbon atoms of residues (thin) are colored as aquamarine (A). 2D representation of ligand 3-GPx4 (2OBI.pdb) interactions with interaction distances (B).

Table 3
EC_{05} and EC_{10} doses of different compounds in SH-SY5Y cells.

	EC_{05} (μM)	EC_{10} (μM)
1	5.71	8.41
2	2.35	3.31
3	2.84	3.65
4	3.38	4.43

The correlation between anticholinesterase and anti-MS effects, as well as correlation between *in silico* and *in vitro* results is a very precious highlight. As a future perspective, further *in vivo* experiments are suggested.

Supplementary material

Supportive figures related to *in silico* activity studies are available in the supplementary material of this article.

CRediT authorship contribution statement

Anil Yilmaz: Writing – review & editing, Writing – original draft, Supervision, Software, Resources, Project administration, Methodology, Investigation, Funding acquisition, Conceptualization. **Murat Koca:** Writing – review & editing, Writing – original draft, Supervision, Software, Resources, Project administration, Methodology, Investigation, Funding acquisition, Conceptualization. **Selami Ercan:** Writing – review & editing, Writing – original draft, Software, Resources, Methodology, Investigation, Funding acquisition. **Ozden Ozgun Acar:** Writing – review & editing, Writing – original draft, Software, Resources, Methodology, Investigation, Funding acquisition. **Mehmet Boga:** Writing – review & editing, Writing – original draft, Software, Resources, Methodology, Investigation, Funding acquisition. **Alaattin Sen:** Writing – review & editing, Writing – original draft, Supervision, Software, Resources, Methodology, Investigation, Funding acquisition. **Adnan Kurt:** Resources, Methodology, Investigation.

Table 4
The expression levels of the selected genes at mRNA level in the SH-SY5Y cell line treated with EC_{05} and EC_{10} doses of compounds **1–4**.

SH-SY5Y Cell Line								
Inflammation/chemokine/cytokine								
	1		**2**		**3**		**4**	
Genes	**EC05**	**EC10**	**EC05**	**EC10**	**EC05**	**EC10**	**EC05**	**EC10**
CCL5	1.02±0.42	-1.28±0.29	1.97±0.07	**5.27±0.13**	1.94±0.07	**2.78±0.22**	1.15±0.08	**2.08±0.35**
CXCL9	-1.48±0.02	**-4.82±0.32**	**2.16±0.16**	1.68±0.18	1.84±0.01	-1.26±0.35	**2.15±0.03**	**3.23±0.33**
CXCL10	-1.57±0.03	**-7.05±0.02**	**2.06±0.17**	1.27±0.61	1.95±0.12	-1.09±0.69	1.83±0.07	**4.12±0.33**
HIF1A	1.62±0.05	-1.57±0.25	1.12±0.72	-1.4±0.33	**2.22±0.01**	1.86±0.11	1.22±0.46	-1.61±0.23
IL6	1.83±0.01	-1.37±0.49	**4.37±0.35**	**2.01±0.24**	1.72±0.27	**2.07±.0.14**	-1.07±0.56	1.14±0.34
NFKB	-1.21±0.22	-1.34±0.32	**2.21±0.08**	**3.03±0.07**	1.57±0.08	**2.55±0.12**	-1.24±0.46	-1.14±0.41
PTPN11	-1.33±0.26	**-2.31±0.05**	1.54±0.22	1.17±0.61	1.54±0.01	**2.52±0.51**	1.01±0.38	-1.05±0.36
STAT3	-1.28±0.19	-1.93±0.07	**2.05±0.11**	**2.32±0.18**	**2.55±0.01**	**2.01±0.01**	-1.17±0.33	-1.21±0.26
TNF-α	-1.55±0.06	**-2.39±0.21**	**2.07±0.24**	**2.27±0.16**	**6.61±0.08**	**2.26±0.21**	**2.41±0.43**	**2.52±0.28**
Myelination/demyelination								
MAG	1.17±0.26	1.08±0.78	1.75±0.19	1.14±0.73	1.05±0.69	-1.33±0.39	1.59±0.48	1.42±0.53
PLP	1.31±0.65	1.74±0.22	1.74±0.35	1.43±0.59	1.84±0.28	-1.36±0.43	1.10±0.62	1.55±0.01
SOD	-1.21±0.17	-1.04±0.75	1.99±0.12	1.62±0.17	**3.54±0.07**	**2.63±0.03**	1.15±0.31	-1.03±0.87
Apoptosis/cell adhesion								
APP	1.43±0.31	-1.46±0.24	1.51±0.44	1.45±0.37	**2.36±0.02**	1.09±0.24	-1.62±0.06	-1.17±0.34
MMP9	**-2.10±0.09**	**-3.34±0.21**	**2.33±0.18**	1.55±0.63	1.67±0.06	1.04±0.71	-1.31±0.41	-1.44±0.33
GFAP	-1.24±0.42	**-2.71±0.51**	**2.41±0.11**	**3.15±0.19**	**8.03±0.54**	**12.6±0.32**	**2.40±0.05**	1.57±0.17

The blue and red colours indicate significantly decreased and increased values, respectively, compared to control values ($p < 0.05$). Results are the Mean ± SD of at least three independent replicates of duplicate measurements.

Declaration of competing interest

The authors declare that they have no known competing financial interests or personal relationships that could have appeared to influence the work reported in this paper.

Data availability

The data that has been used is confidential.

Acknowledgments

The authors would like to thank to Trakya University, Adiyaman University, Batman University, Dicle University, Pamukkale University, and the University of Abdullah Gul.

Supplementary materials

Supplementary material associated with this article can be found, in the online version, at doi:10.1016/j.molstruc.2024.139193.

References

[1] M. Prince, R. Bryce, E. Albanese, A. Wimo, W. Ribeiro, C.P. Ferri, The global prevalence of dementia: a systematic review and metaanalysis, Alzheimers Dement 9 (1) (2013) 63–75, https://doi.org/10.1016/j.jalz.2012.11.007.
[2] A. Burns, S. Iliffe, Alzheimer's disease, BMJ 338 (2009) b158, https://doi.org/10.1136/bmj.b158.
[3] M. Citron, Beta-secretase as a target for the treatment of Alzheimer's disease, J. Neurosci. Res. 70 (3) (2002) 373–379, https://doi.org/10.1002/jnr.10393.
[4] J.L. Cummings, The role of cholinergic agents in the management of behavioural disturbances in Alzheimer's disease, Int. J. Neuropsychopharmacol. 3 (2) (2000) 21–29, https://doi.org/10.1093/ijnp/3.Supplement_2.S21.
[5] A. Yilmaz, P. Caglar, T. Dirmenci, N. Goren, G. Topcu, A novel Isopimarane diterpenoid with acetylcholinesterase inhibitory activity from nepeta sorgerae, an endemic species to the nemrut mountain, Nat. Prod. Commun. 7 (6) (2012) 693–696.
[6] A. Yilmaz, M. Boga, G. Topcu, Novel terpenoids with potential anti-Alzheimer activity from Nepeta obtusicrena, Rec. Nat. Prod. 10 (5) (2016) 530–541.
[7] F. Vafadarnejad, M. Saeedi, M. Mahdavi, A. Rafinejad, E. Karimpour-Razkenari, B. Sameem, M. Khanavi, T. Akbarzadeh, Novel Indole-Isoxazole hybrids: synthesis and in vitro anti-cholinesterase activity, Lett. Drug. Des. Discov. 14 (6) (2017) 712–717, https://doi.org/10.2174/1570180813666161018124726.
[8] K.O. Yerdelen, M. Koca, Z. Kasap, B. Anil, Preparation, anticholinesterase activity, and docking study of new 2-butenediamide and oxalamide derivatives, J. Enz. Inhib. Med. Chem. 30 (4) (2015) 671–678, https://doi.org/10.3109/14756366.2014.959947.
[9] J.L. Sussman, M. Harel, F. Frolow, C. Oefner, A. Goldman, L. Toker, I. Silman, Atomic structure of acetylcholinesterase from Torpedo californica: a prototypic acetylcholine-binding protein, Science (1979) 253 (5022) (1991) 872–879, https://doi.org/10.1126/science.1678899.
[10] R.J. Flower, The development of COX2 inhibitors, Nat. Rev. Drug Discov. 2 (3) (2003) 179–191, https://doi.org/10.1038/nrd1034.
[11] M. Nivsarkar, A. Banerjee, H. Padh, Cyclooxygenase inhibitors: a novel direction for Alzheimer's management, Pharmacol. Rep. 60 (5) (2008) 692–698.
[12] K. Yasojima, W.W. Tourtellotte, E.G. McGeer, P.L. McGeer, Marked increase in cyclooxygenase-2 in ALS spinal cord: implications for therapy, Neurology 57 (6) (2001) 952–956, https://doi.org/10.1212/wnl.57.6.952.
[13] B.J. Al-Hourani, S.K. Sharma, J.Y. Mane, J. Tuszynski, V. Baracos, T. Kniess, M. Suresh, J. Pietzsch, F. Wuest, Synthesis and evaluation of 1,5-diaryl-substituted tetrazoles as novel selective cyclooxygenase-2 (COX-2) inhibitors, Bioorg. Med. Chem. Lett. 21 (6) (2011) 1823–1826, https://doi.org/10.1016/j.bmcl.2011.01.057.
[14] J.K. Dhanjal, A.K. Sreenidhi, K. Bafna, S.P. Katiyar, S. Goyal, A. Grover, D. Sundar, Computational structure-based de novo design of hypothetical inhibitors against the anti- inflammatory target COX-2, PLoS One 10 (8) (2015) e0134691, https://doi.org/10.1371/journal.pone.0134691.
[15] A. Zarghi, S. Arfaei, Selective COX-2 inhibitors: a review of their structure-activity relationships, Iran J. Pharm. Res. 10 (4) (2011) 655–683.
[16] N. Razzaghi-Asl, S. Mirzayi, K. Mahnam, S. Sepehri, Identification of COX-2 inhibitors via structure-based virtual screening and molecular dynamics simulation, J. Mol. Graph Model. 83 (2018) 138–152, https://doi.org/10.1016/j.jmgm.2018.05.010.
[17] A.T. Bender, J.A. Beavo, Cyclic nucleotide phosphodiesterases: molecular regulation to clinical use, Pharmacol. Rev. 58 (3) (2006) 488–520, https://doi.org/10.1124/pr.58.3.5.
[18] J. Felding, M.D. Sørensen, T.D. Poulsen, J. Larsen, C. Andersson, P. Refer, K. Engell, L.G. Ladefoged, T. Thormann, A.M. Vinggaard, P. Hegardt, A. Søhoel, S.F. Nielsen, Discovery and early clinical development of 2-6-[2-(3,5-dichloro-4-pyridyl)acetyl]-2,3-dimethoxyphenoxy-N-propylacetamide (LEO 29102), a soft-drug inhibitor of phosphodiesterase 4 for topical treatment of atopic dermatitis, J. Med. Chem. 57 (14) (2014) 5893–5903, https://doi.org/10.1021/jm500378a.
[19] N. Bartke, Y.A. Hannun, Bioactive sphingolipids: metabolism and function, J. Lipid Res. 50 (2009) S91–S96, https://doi.org/10.1194/jlr.R800080-JLR200.
[20] N.C. Hait, J. Allegood, M. Maceyka, G.M. Strub, K.B. Harikumar, S.K. Singh, C. Luo, R. Marmorstein, T. Kordula, S. Milstien, S. Spiegel, Regulation of histone

acetylation in the nucleus by sphingosine-1-phosphate, Science (1979) 325 (5945) (2009) 1254–1257, https://doi.org/10.1126/science.1176709.
[21] M. Matloubian, C.G. Lo, G. Cinamon, M.J. Lesneski, Y. Xu, V. Brinkmann, M. L. Allende, R.L. Proia, J.G. Cyster, Lymphocyte egress from thymus and peripheral lymphoid organs is dependent on S1P receptor 1, Nature 427 (6972) (2004) 355–360, https://doi.org/10.1038/nature02284.
[22] M. Serra, J.D. Saba, Sphingosine 1-phosphate lyase, a key regulator of sphingosine 1-phosphate signaling and function, Adv. Enz. Regul. 50 (1) (2010) 349–362, https://doi.org/10.1016/j.advenzreg.2009.10.024.
[23] S.R. Schwab, J.P. Pereira, M. Matloubian, Y. Xu, Y. Huang, J.G. Cyster, Lymphocyte sequestration through S1P lyase inhibition and disruption of S1P gradients, Science (1979) 309 (5741) (2005) 1735–1739, https://doi.org/10.1126/science.1113640.
[24] P. Vogel, M.S. Donoviel, R. Read, G.M. Hansen, J. Hazlewood, S.J. Anderson, W. Sun, J. Swaffield, T. Oravecz, Incomplete inhibition of sphingosine 1-phosphate lyase modulates immune system function yet prevents early lethality and non-lymphoid lesions, PLoS One 4 (1) (2009) e4112, https://doi.org/10.1371/journal.pone.0004112.
[25] I. Karaca, I.Y. Tamboli, K. Glebov, J. Richter, L.H. Fell, M.O. Grimm, V. J. Haupenthal, T. Hartmann, M.H. Gräler, G. van Echten-Deckert, J. Walter, Deficiency of sphingosine-1-phosphate lyase impairs lysosomal metabolism of the amyloid precursor protein, J. Biol. Chem. 289 (24) (2014) 16761–16772, https://doi.org/10.1074/jbc.M113.535500.
[26] B. Oskouian, P. Sooriyakumaran, A.D. Borowsky, A. Crans, L. Dillard-Telm, Y. Y. Tam, P. Bandhuvula, J.D. Saba, Sphingosine-1-phosphate lyase potentiates apoptosis via p53- and p38-dependent pathways and is down-regulated in colon cancer, Proc. Natl. Acad. Sci. U. S. A. 103 (46) (2006) 17384–17389, https://doi.org/10.1073/pnas.0600050103.
[27] I.A. Gorshkova, H. Wang, G.A. Orbelyan, J. Goya, V. Natarajan, D.G. Beiser, T.L. V. Hoek, E.V. Berdyshev, Inhibition of sphingosine-1-phosphate lyase rescues sphingosine kinase-1-knockout phenotype following murine cardiac arrest, Life Sci 93 (9–11) (2013) 359–366, https://doi.org/10.1016/j.lfs.2013.07.017.
[28] A. Billich, T. Baumruker, C. Beerli, M. Bigaud, C. Bruns, T. Calzascia, A. Isken, B. Kinzel, E. Loetscher, B. Metzler, M. Mueller, B. Nuesslein-Hildesheim, B. Kleylein-Sohn, Partial deficiency of sphingosine-1-phosphate lyase confers protection in experimental autoimmune encephalomyelitis, PLoS One 8 (3) (2013) e59630, https://doi.org/10.1371/journal.pone.0059630.
[29] M.J. Pulkoski-Gross, J.C. Donaldson, L.M. Obeid, Sphingosine-1-phosphate metabolism: a structural perspective, Crit. Rev. Biochem. Mol. Biol. 50 (4) (2015) 298–313, https://doi.org/10.3109/10409238.2015.1039115.
[30] B.K. Tsang, R. Macdonell, Multiple sclerosis- diagnosis, management and prognosis, Aust. Fam. Phys. 40 (12) (2011) 948–955.
[31] C. Ge, S. Zhang, H. Mu, S. Zheng, Z. Tan, X. Huang, C. Xu, J. Zou, Y. Zhu, D. Feng, J. Aa, Emerging mechanisms and disease implications of ferroptosis: potential applications of natural products, Front. Cell. Dev. Biol. 9 (2021) 774957, https://doi.org/10.3389/fcell.2021.774957.
[32] H-f. Yan, T. Zou, Q-z. Tuo, S. Xu, H. Li, A.A. Belaidi, P. Lei, Ferroptosis: mechanisms and links with diseases, Signal Transduct. Target Ther. 6 (1) (2021) 49, https://doi.org/10.1038/s41392-020-00428-9.
[33] B. Adamczyk, M. Adamczyk-Sowa, New insights into the role of oxidative stress mechanisms in the pathophysiology and treatment of multiple sclerosis, Oxid. Med. Cell Longev. 2016 (2016) 1973834, https://doi.org/10.1155/2016/1973834.
[34] W.S. Yang, B.R. Stockwell, Ferroptosis: death by lipid peroxidation, Trends. Cell Biol 26 (3) (2016) 165–176, https://doi.org/10.1016/j.tcb.2015.10.014.
[35] A.A. Alameen, M. Abdalla, H.M. Alshibl, M.R. AlOthman, M.M. Alkhulaifi, T. O. Mirgany, R. Elsayim, In-silico studies of glutathione peroxidase4 activators as candidate for multiple sclerosis management, J. Saudi Chem. Soc. 26 (6) (2022) 101554, https://doi.org/10.1016/j.jscs.2022.101554.
[36] A. Yilmaz, M. Koca, M. Boga, A. Kurt, T. Ozturk, Synthesis of novel oxime and benzofuran chemical frameworks possessing potent anticholinesterase activity: a sar study related to alzheimer disease, ChemistrySelect. 8 (30) (2023) e202302058, https://doi.org/10.1002/slct.202302058.
[37] ChemAxon, Marvin (2017).
[38] BIOVIA, Discovery visualizer studio, v21.1.0.20298. Dassault Systèmes, Dassault Systèmes, San Diego, 2021.
[39] E. Anders, R. Koch, P. Freunscht, Optimization and application of lithium parameters for PM3, J. Comput. Chem. 14 (11) (1993) 1301–1312, https://doi.org/10.1002/jcc.540141106.
[40] M.J.S. Dewar, E.G. Zoebisch, E.F. Healy, J.J.P. Stewart, Development and use of quantum mechanical molecular models. 76. AM1: a new general purpose quantum mechanical molecular model, J. Amer. Chem. Soc. 107 (13) (1985) 3902–3909, https://doi.org/10.1021/ja00299a024.
[41] A.D. Becke, Density-functional thermochemistry. 3. the role of exact exchange, J. Chem. Phys. 98 (7) (1993) 5648–5652, https://doi.org/10.1063/1.464913.
[42] C.T. Lee, W.T. Yang, R.G. Parr, Development of the colle-salvetti correlation-energy formula into a functional of the electron-density, Phys. Rev. B. 37 (2) (1988) 785–789, https://doi.org/10.1103/PhysRevB.37.785.
[43] J. Cheung, M.J. Rudolph, F. Burshteyn, M.S. Cassidy, E.N. Gary, J. Love, M. C. Franklin, J.J. Height, Structures of human acetylcholinesterase in complex with pharmacologically important ligands, J. Med. Chem. 55 (22) (2012) 10282–10286, https://doi.org/10.1021/jm300871x.
[44] A. Meden, D. Knez, M. Jukič, X. Brazzolotto, M. Gršič, A. Pišlar, A. Zahirović, J. Kos, F. Nachon, J. Svete, S. Gobec, U. Grošelj, Tryptophan-derived butyrylcholinesterase inhibitors as promising leads against Alzheimer's disease, Chem. Commun. (Camb). 55 (26) (2019) 3765–3768, https://doi.org/10.1039/c9cc01330j.
[45] J.L. Wang, D. Limburg, M.J. Graneto, J. Springer, J.R.B. Hamper, S. Liao, J. L. Pawlitz, R.G. Kurumbail, T. Maziasz, J.J. Talley, J.R. Kiefer, J. Carter, The novel benzopyran class of selective cyclooxygenase-2 inhibitors. Part 2: the second clinical candidate having a shorter and favorable human half-life, Bioorg. Med. Chem. Lett. 20 (23) (2010) 7159–7163, https://doi.org/10.1016/j.bmcl.2010.07.054.
[46] S. Weiler, N. Braendlin, C. Beerli, C. Bergsdorf, A. Schubart, H. Srinivas, B. Oberhauser, A. Billich, Orally active 7-substituted (4-benzylphthalazin-1-yl)-2-methylpiperazin-1-yl]nicotinonitriles as active-site inhibitors of sphingosine 1-phosphate lyase for the treatment of multiple sclerosis, J. Med. Chem. 57 (12) (2014) 5074–5084, https://doi.org/10.1021/jm500338n.
[47] P. Scheerer, A. Borchert, N. Krauss, H. Wessner, C. Gerth, W. Höhne, H. Kuhn, Structural basis for catalytic activity and enzyme polymerization of phospholipid hydroperoxide glutathione peroxidase-4 (GPx4), Biochemistry 46 (31) (2007) 9041–9049, https://doi.org/10.1021/bi700840d.
[48] H.M. Berman, J. Westbrook, Z. Feng, G. Gilliland, T.N. Bhat, H. Weissig, I. N. Shindyalov, P.E. Bourne, The protein data bank, Nucl. Acids Res 28 (1) (2000) 235–242, https://doi.org/10.1093/nar/28.1.235.
[49] G.M. Morris, R. Huey, W. Lindstrom, M.F. Sanner, R.K. Belew, D.S. Goodsell, A. J. Olson, AutoDock4 and AutoDockTools4: automated docking with selective receptor flexibility, J. Comput. Chem. 30 (16) (2009) 2785–2791, https://doi.org/10.1002/jcc.21256.
[50] S. Ercan, E. Çınar, A molecular docking study of potential inhibitors and repurposed drugs against SARS-CoV-2 main protease enzyme, J. Ind Chem. Soc. 98 (3) (2021) 100041, https://doi.org/10.1016/j.jics.2021.100041.
[51] O. Ozgun-Acar, I. Gazioglu, Ufuk Kolak, A. Sen, G. Topcu, A potential therapeutic role in multiple sclerosis for stigmast-5,22-dien-3β-ol myristate isolated from Capparis ovata, Eurobiotech. J. 1 (3) (2017) 241–246, https://doi.org/10.24190/ISSN2564-615X/2017/03.08.
[52] E.M. Terefe, A. Ghosh, Molecular docking, validation, dynamics simulations, and pharmacokinetic prediction of phytochemicals isolated from croton dichogamus against the HIV-1 reverse transcriptase, Bioinform. Biol. Insig. 16 (2022) 117793222211256, https://doi.org/10.1177/11779322221125605.
[53] D. Ramírez, J. Caballero, Is it reliable to take the molecular docking top scoring position as the best solution without considering available structural data? Molecules 23 (5) (2018) 1038, https://doi.org/10.3390/molecules23051038.
[54] K.J. Livak, T.D. Schmittgen, Analysis of relative gene expression data using real-time quantitative PCR and the 2(-Delta Delta C(T)) Method, Methods 25 (4) (2001) 402–408, https://doi.org/10.1006/meth.2001.1262.
[55] R.H. Quarles, Myelin-associated glycoprotein (MAG): past, present and beyond, J. Neurochem. 100 (6) (2007) 1431–1448, https://doi.org/10.1111/j.1471-4159.2006.04319.x.
[56] O. Ozgun-Acar, G. Celik-Turgut, I. Gazioglu, U. Kolak, S. Ozbal, B.U. Ergur, S. Arslan, A. Sen, G. Topcu, Capparis ovata treatment suppresses inflammatory cytokine expression and ameliorates experimental allergic encephalomyelitis model of multiple sclerosis in C57BL/6 mice, J. Neuroimmunol. 298 (2016) 106–116, https://doi.org/10.1016/j.jneuroim.2016.07.010.
[57] S.M. Leibowitz, J. Yan, NF-κB pathways in the pathogenesis of multiple sclerosis and the therapeutic implications, Front. Mol. Neurosci. 9 (2016) 1–23, https://doi.org/10.3389/fnmol.2016.00084.
[58] M. Boziki, N. Grigoriadis, An update on the role of matrix metalloproteinases in the pathogenesis of multiple sclerosis, Med. Chem. 14 (2) (2017) 155–169, https://doi.org/10.2174/1573406413666170906122803.
[59] E. Miller, M. Mrowicka, K. Malinowska, J. Mrowicki, J. Saluk-Juszczak, J. Kedziora, The effects of whole-body cryotherapy on oxidative stress in multiple sclerosis patients, J. Therm. Biol 35 (8) (2010) 406–410, https://doi.org/10.1016/j.jtherbio.2010.08.006.